

Supplement of Atmos. Chem. Phys., 14, 8483–8499, 2014
<http://www.atmos-chem-phys.net/14/8483/2014/>
doi:10.5194/acp-14-8483-2014-supplement
© Author(s) 2014. CC Attribution 3.0 License.



Supplement of

Impact of external industrial sources on the regional and local SO₂ and O₃ levels of the Mexico megacity

V. H. Almanza et al.

Correspondence to: G. Sosa (gsosa@imp.mx)

Supplementary Material

In this supplement the results of additional simulations considering the aerosol phase are presented.

To address the inclusion of aerosols, our original model configuration had to be modified in order to consider the aerosol chemistry. Fast et al (2009) mentioned that treatments for aqueous chemistry, cloud-aerosol interactions, aerosol indirect effects, and wet deposition could have been important after the third cold surge. For this reason we considered worthwhile to include these processes in our aerosol simulations. These model parameterizations require the Goddard scheme for the shortwave radiation module; however, in our original model configuration we used the Dudhia scheme. Thus, the objective of these simulations using the Goddard scheme is to determine the effect of including the aerosol module on the modeled average SO_2 and ozone concentrations. We used the MOSAIC module with 4 bins in order to reduce computing time.

This supplement is organized as follows. Section 1 presents the results with the inclusion of the aerosol phase in WRF-Chem. Section 2 presents the results of the effect of the aerosol phase on the contribution of cement plants. Section 3 briefly addresses the reduction scenario S5. Finally Section 5 presents the results for the regional ozone levels.

1. Inclusion of the aerosol phase

A new baseline case for the gas phase was constructed. The difference with the baseline case reported in the manuscript is that the Goddard scheme for the shortwave radiation was used instead of the Dudhia scheme. The purpose of the simulations was to better depict the influence of the aerosol phase on the modeled average SO₂ concentration. The same input files for both the emissions inventory and Multiscale Four Dimensional Data Assimilation (FDDA) that were used in the original configuration were also used in all the aerosol simulations. Just for consistency purposes, it was decided to also include aerosol simulations without the inclusion of direct and indirect effects to better depict the influence of the aerosol module on the modeled concentration. It is important to mention that we are not attempting to quantify either the direct or the indirect effect. It is beyond the scope of this work. Results are presented in Figure 1.

Figure 1 shows the estimated average SO₂ concentration during the simulation period for the considered simulation cases. The notation is as follows: **BCg** denotes the original baseline case configuration for the gas phase which was presented in the manuscript; **BCa** denotes the original baseline case configuration presented in the manuscript but with the aerosol phase turned on; **BCGg** denotes the new baseline case configuration for the gas phase using the Goddard shortwave radiation scheme; **BCGa** denotes the configuration using the Goddard shortwave radiation scheme with the aerosol phase turned on; and **BCGs** denotes the configuration using the Goddard shortwave radiation scheme plus the inclusion of the aerosol direct and indirect effects. **OBS** denotes the average observed concentration at each monitoring site.

After including the aerosol phase in WRF-Chem and comparing the simulations with respect to the baseline case configuration, the results suggested a slight increase in the model average SO₂ concentrations in most of the monitoring stations. However, in the northwest region the average SO₂ concentration slightly decreased (BCa). When using the Goddard scheme (BCGa), the SO₂ concentration also decreased in the northwest and in the southwest region as well. Nevertheless, it slightly increased in the northeast and southeast regions of the basin. In contrast, after including the direct and indirect effect (BCGs), the average concentration tended to increase in the northwest, and in part of the center and southwest regions. Even though the average concentration slightly increased in some regions of the basin, the resulting magnitude in all the simulation cases was relatively comparable to the results presented in the manuscript. This is better depicted in Figure 2. The figure shows the results when taking the arithmetic difference between the average concentrations obtained after including the aerosol phase and those obtained with the gas phase. The notation in Figure 2 is as follows: **BCag** denotes the difference between the results with aerosol phase and the results with the gas phase using the Dudhia scheme of shortwave radiation; **BCGag** denotes the same difference as in the previous case but using the Goddard scheme of shortwave radiation; **BCGsg** denotes the difference when including the aerosol direct and indirect effects using the Goddard scheme. The last three plots are included to show the difference between the results of all the cases using the Goddard scheme and the original results presented in the manuscript. Thus, the notation is similar: **BCGg-BCg** denotes the difference between the two baseline cases; **BCGa-BCg** is the

difference between the aerosol phase case and the baseline case of the manuscript and **BCGs-BCg** is the difference between the case including the aerosol direct and indirect effects and the baseline case.

The differences in average SO₂ concentration range from about -0.3 ppb and 0.5 ppb, with some stations having differences of about 1 ppb. The median for all the simulation cases is about 0.2 ppb, which roughly represents a 10 % difference.

Since the radiation scheme also affects the PBL module, the inclusion of the Goddard scheme resulted in higher variability in the average SO₂ concentration as the last three boxplots suggest. In general, the inclusion of the aerosol module resulted in lower PBLs; however the Goddard scheme plus the direct and indirect effects tended to give higher PBLs on the regional scale with respect to the baseline case using Dudhia scheme and to the baseline case using the Goddard scheme. Therefore, part of the increase on the average concentration can be attributed to the shallow PBLs obtained with the Goddard scheme.

The chemical mechanism is also contributing to the observed differences. The Multiscale FDDA can also influence the model performance since it can affect the feedback processes (Forkel et al. 2012). In addition, the original results included a preliminary sensitivity analysis using the Dudhia scheme on nudging coefficients and the calculation of diffusion in physical space for the innermost domain. The main result of that sensitivity analysis was to activate the convective parameterization in the innermost domain. This implies that a similar sensitivity analysis using the Goddard scheme would have to be performed in order to determine more precisely the influence of those parameters in the final model configuration. For instance, we observed that the variability in modeled temperature increased after using the Goddard scheme and the aerosol module since the bias and MAE presented a slight increase. Wind speed performance was similar in all simulation cases; however, the model performance in wind direction tended to have higher variability. Using the Goddard scheme resulted in one hour delay in the timing of the simulated SO₂ concentration peak on 23 March at some monitoring stations (Figure 3).

Karidys et al. (2011) report a sulfate concentration of about 25 ug/m³. They used PMCAMx-2008 with SAPRC99 for the period of March 10-31 2006. Despite the differences in the modeling setup and the effect of the Goddard scheme and aerosol module on the model performance, our results also suggest concentrations of PM₁ sulfate of about 23 ug/m³ to 25 ug/m³ over the Tula Industrial Complex as shown in Figure 4. We observed that neglecting the direct and indirect effects in the model configuration resulted in slightly lower PM₁ sulfate concentration on the regional level.

2. Cement plants

As described above, we used the model configuration which included the aerosol direct and indirect effects. Figure 5 presents the results obtained with the configuration reported in the manuscript (top panel) and the configuration with aerosol chemistry (bottom panel).

The results suggest that when using the aerosol chemistry T1 had the highest SO₂ contribution from cement plants emissions during the simulation period, whereas in the original results the highest contribution was estimated at VIF station. That is, the average contribution at T1 increased from 41 % to 52 %. In general, it was observed an increment ranging from 2 % to 10 % in the contribution from TIC; a decrement ranging from -1% to -15% in the MCMA contribution and an increment ranging from 1 % to 10 % in the cement plants contribution with respect to the original results. Thus, the inclusion of the aerosol chemistry in the simulations suggested that the contribution of the TIC and the cement plants emissions to SO₂ levels could be higher and that the contribution of urban emission sources could be lower. It is important to mention that there was a consistent overprediction on 23 March and on 25 March in all the simulations with the aerosol chemistry as shown in Figure 3. The resulting magnitude was higher than the one obtained with the original configuration in most of the monitoring stations. It was observed that the model predicted a convergence zone in the original results from 17:00 LST to 21:00 LST on 24 March which prevented the plume to be transported farther to the south (Figure 6). The convergence zone extended roughly from the upper region of the western ridge to northern T1. Once the convergence zone disappeared, the plume entered farther to the northwest. This convergence zone was also present in the simulations with the aerosol phase; however, it extended to a greater area than in the original results which resulted in slightly longer time for the plume to be transported to the south. Thus, the combined effect of a shallow PBL and a wider convergence zone promoted higher SO₂ concentrations.

Therefore, the results including the aerosol phase are relatively similar to those from the gas phase. Even though the magnitude of the contributions changed, the findings reported in the manuscript are not modified substantially, since both configurations suggest that the cement plants contribute mainly in the northeast and part of the southeast regions of the basin.

3. Emissions reduction scenario S5

The influence of the aerosol phase was also investigated for the emissions reduction scenarios, focusing on the S5 scenario which includes the reduction in both external and local sources. The simulations included the aerosol phase plus the direct and indirect effects. Figure 7 shows that results with the aerosol phase are in agreement with those reported in the manuscript. The differences in contribution percentages range from -1.5 to 6; however, after the inclusion of the aerosol phase it is still suggested that the combined reduction in external and local sources would be more efficient for reducing the SO₂ levels in the basin. In addition, the southern region would be more sensitive to this set of reductions. Thus, our assumption of a small influence of the aerosol phase in model results for SO₂ is likely to not affect the main findings reported in the manuscript for the contribution of external sources and in the emissions reduction scenarios.

4. Regional ozone

It was observed that after including the aerosol phase the variability in the ozone model concentration was higher than in the SO₂ model concentration. In this case, the meteorology exerted greater influence on the transport of precursors so that larger differences in the spatial distribution were present for the ozone plume. When comparing the baseline cases for the gas phase on 25 March, the results using the Goddard scheme presented slightly higher concentrations in the basin than the results obtained with the Dudhia scheme. In the late afternoon, the ozone plume from TIC-generated precursors using the Goddard scheme reached the southern part of the basin; whilst with the Dudhia scheme the ozone plume tended to remain more in the north region of the basin (Figure 8).

Even though these differences in the spatial distribution resulted in low concentrations, the effect of meteorology on the ozone plume transport was enhanced when including the aerosol phase. Basically, the highly coupled feedback effects resulted in changes in wind direction that promoted a slightly different ozone distribution between the simulation case considering all the point sources and the simulation case without TIC-generated precursors (Figure 9). This resulted in regions with either high or low difference in ozone concentration. However, the average difference for the entire period between the simulation with aerosol phase and the baseline case reported in the manuscript is of about ± 5 ppb (Figure 10).

The inclusion of the aerosol phase suggests that the impact of the TIC-generated precursors to the regional ozone levels could decrease in magnitude in the eastern and southern regions in the State of Hidalgo for this simulation period; and could increase in magnitude in the northwest region of the MCMA. Nevertheless, a main finding in the original results was that the suggested highest contribution from the TIC occurred on 25 March. A similar result is obtained after including the aerosol phase as shown in Figure 11. Thus, despite the spatial variability the results including the aerosol phase are comparable to the original results in the manuscript obtained with the gas phase.

It can be concluded that the average concentrations of sulfur dioxide and ozone are not substantially modified after the inclusion of the aerosol phase in the model simulations for this period. For this reason, we consider that our first results are sufficiently reliable to support the discussion of this work.

References

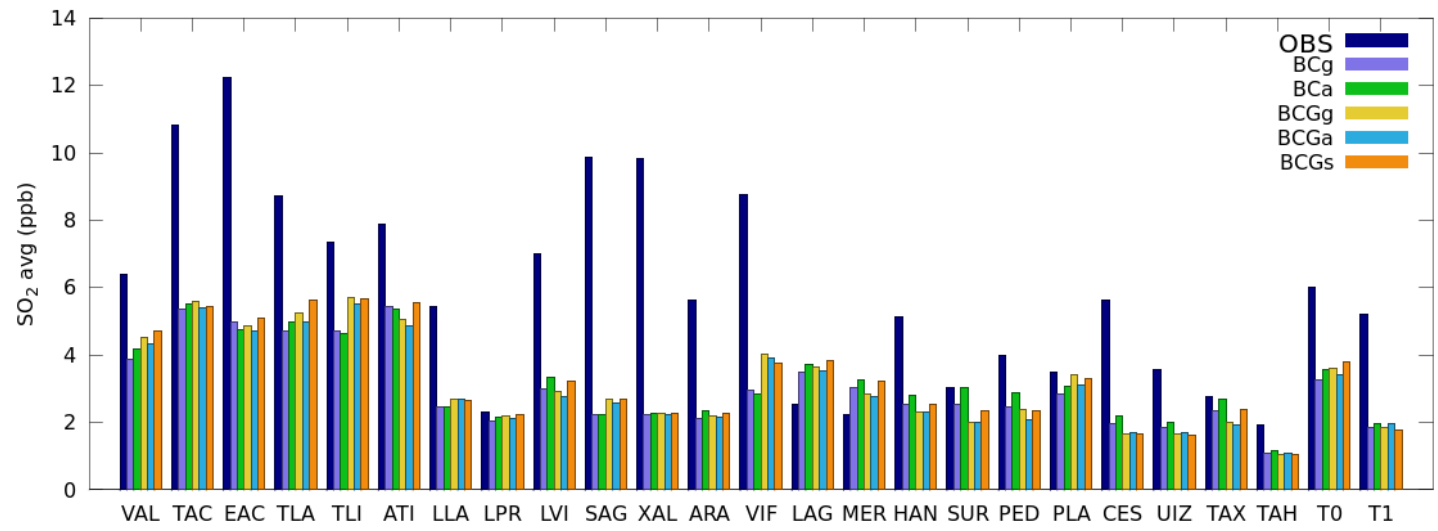
de Foy, B., Krotkov, N. A., Bei, N., Herndon, S. C., Huey, L. G., Martínez, A.-P., Ruiz-Suárez, L. G., Wood, E. C., Zavala, M., and Molina, L. T.: Hit from both sides: tracking industrial and volcanic plumes in Mexico City with surface measurements and OMI SO₂ retrievals during the MILAGRO field campaign, *Atmos. Chem. Phys.*, 9, 9599-9617, doi:10.5194/acp-6-2321-2006, 2009a.

Fast, J. D., de Foy, B., Acevedo Rosas, F., Caetano, E., Carmichael, G., Emmons, L., McKenna, D., Mena, M., Skamarock, W., Tie, X., Coulter, R. L., Barnard, J. C., Wiedinmyer, C., and Madronich, S.: A

meteorological overview of the MILAGRO field campaigns, *Atmos. Chem. Phys.*, 7, 2233-2257, doi:10.5194/acp-7-2233-2007, 2007.

Fast, J. D., Aiken, A. C., Allan, J., Alexander, L., Campos, T., Canagaratna, M. R., Chapman, E., DeCarlo, P. F., de Foy, B., Gaffney, J., de Gouw, J., Doran, J. C., Emmons, L., Hodzic, A., Herndon, S. C., Huey, G., Jayne, J. T., Jimenez, J. L., Kleinman, L., Kuster, W., Marley, N., Russell, L., Ochoa, C., Onasch, T. B., Pekour, M., Song, C., Ulbrich, I. M., Warneke, C., Welsh-Bon, D., Wiedinmyer, C., Worsnop, D. R., Yu, X.-Y., and Zaveri, R.: Evaluating simulated primary anthropogenic and biomass burning organic aerosols during MILAGRO: implications for assessing treatments of secondary organic aerosols, *Atmos. Chem. Phys.*, 9, 6191-6215, doi:10.5194/acp-9-6191-2009, 2009.

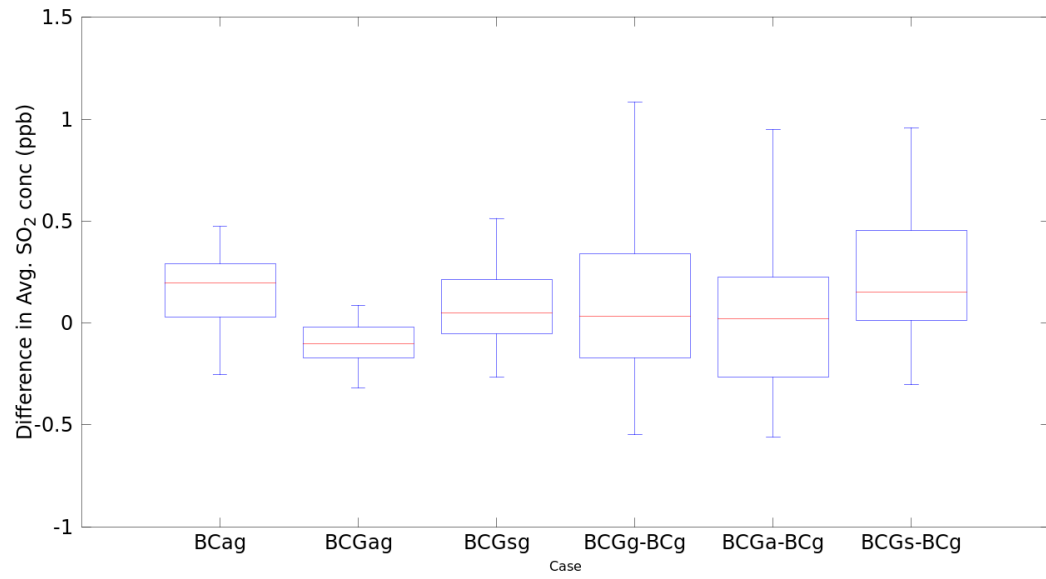
Forkel, R., Werhahn, J., Hansen, A. B., McKeen, S., Peckham, S., Grell, G., and Suppan, P.: Effect of aerosol-radiation feedback on regional air quality – A case study with WRF/Chem, *Atmospheric Environment*, 53, 202 – 211, 2012.



1

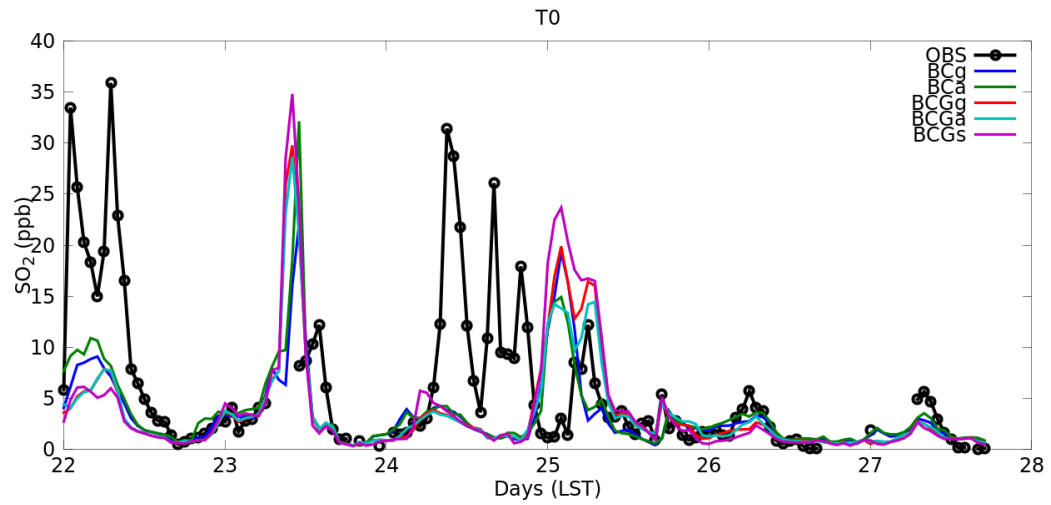
2 **Figure 1. Average SO₂ concentration after including the aerosol phase.**

1



2
3
4
5

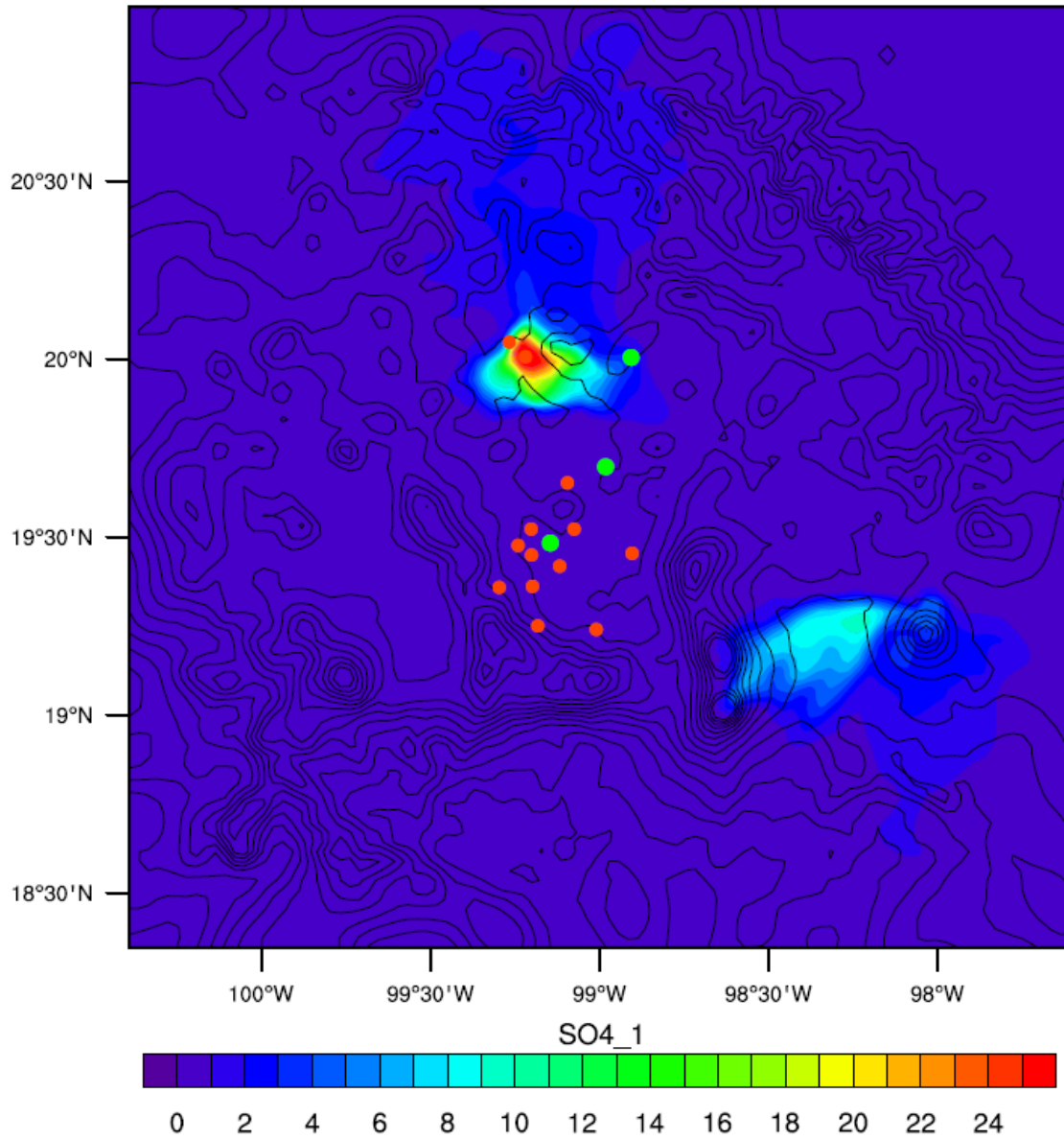
Figure 2. Boxplot of differences in the average SO₂ concentration for the considered simulation cases.



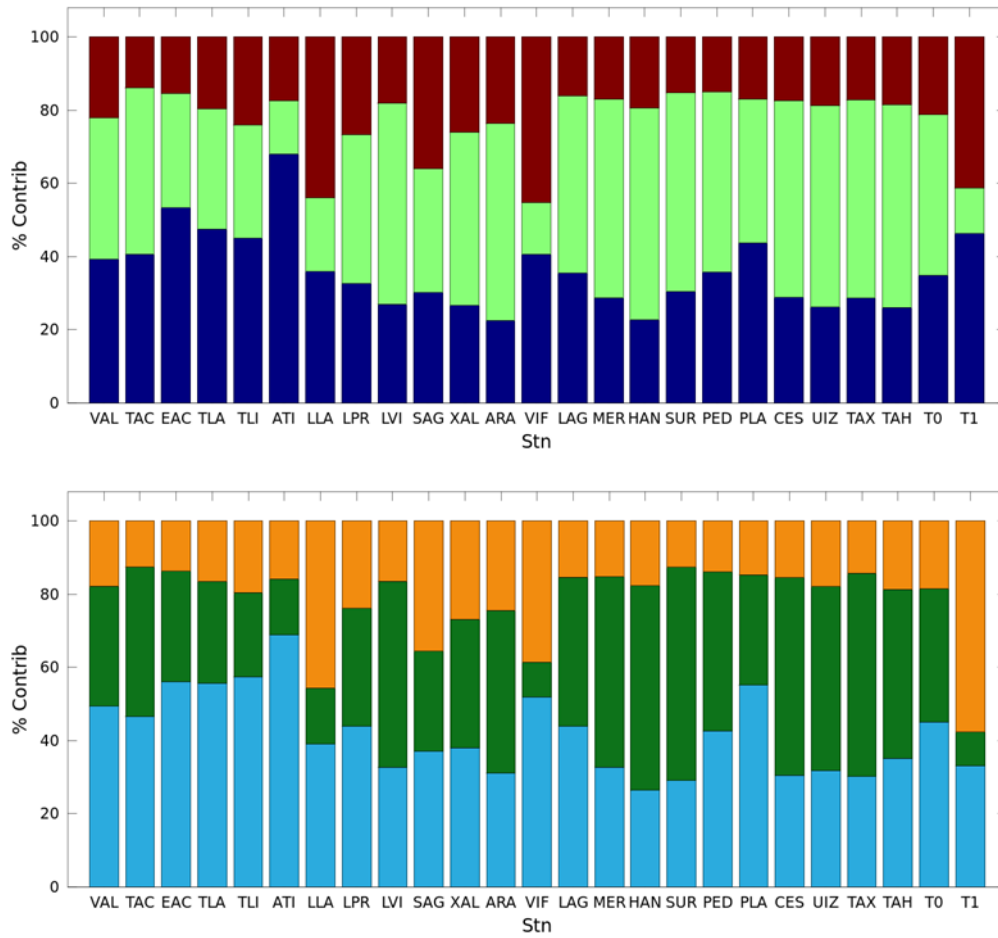
1
2
3
4

Figure 3. Time series of SO₂ concentration at T0 for the simulation cases considering the aerosol phase.

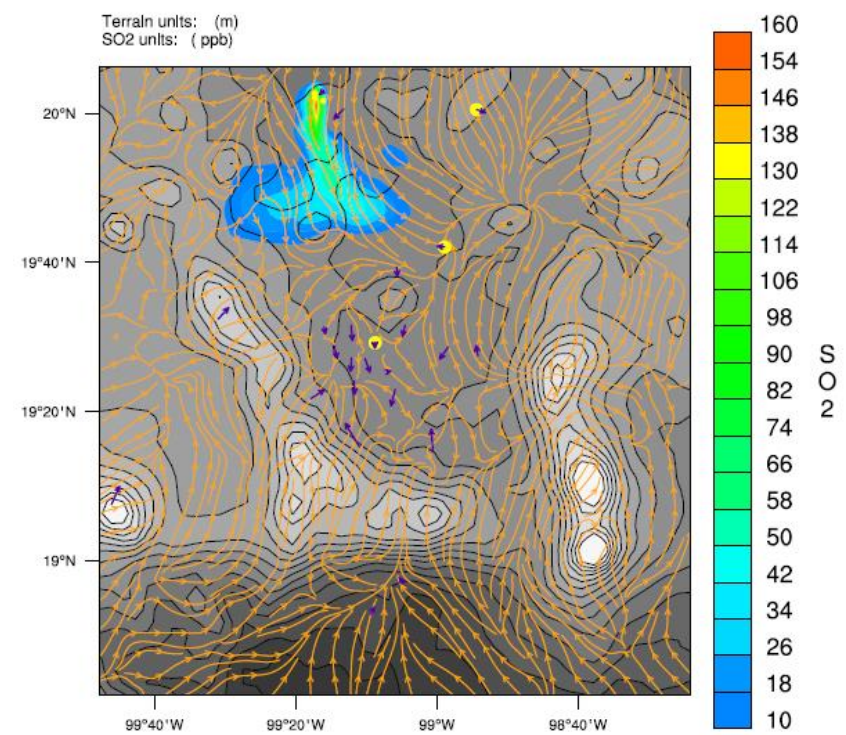
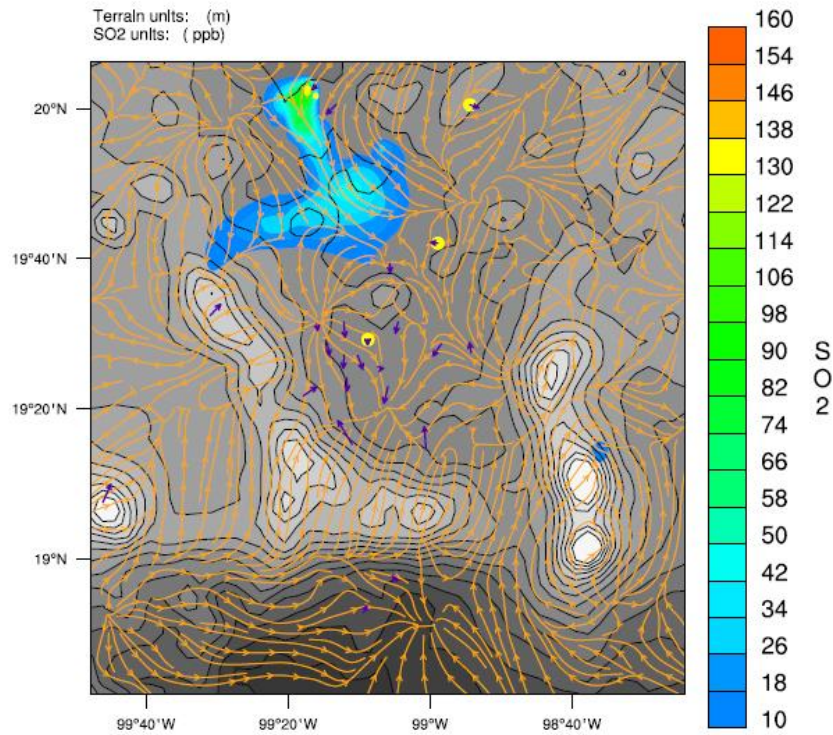
Terrain units: (m)
SO4 units: (ug / m3)



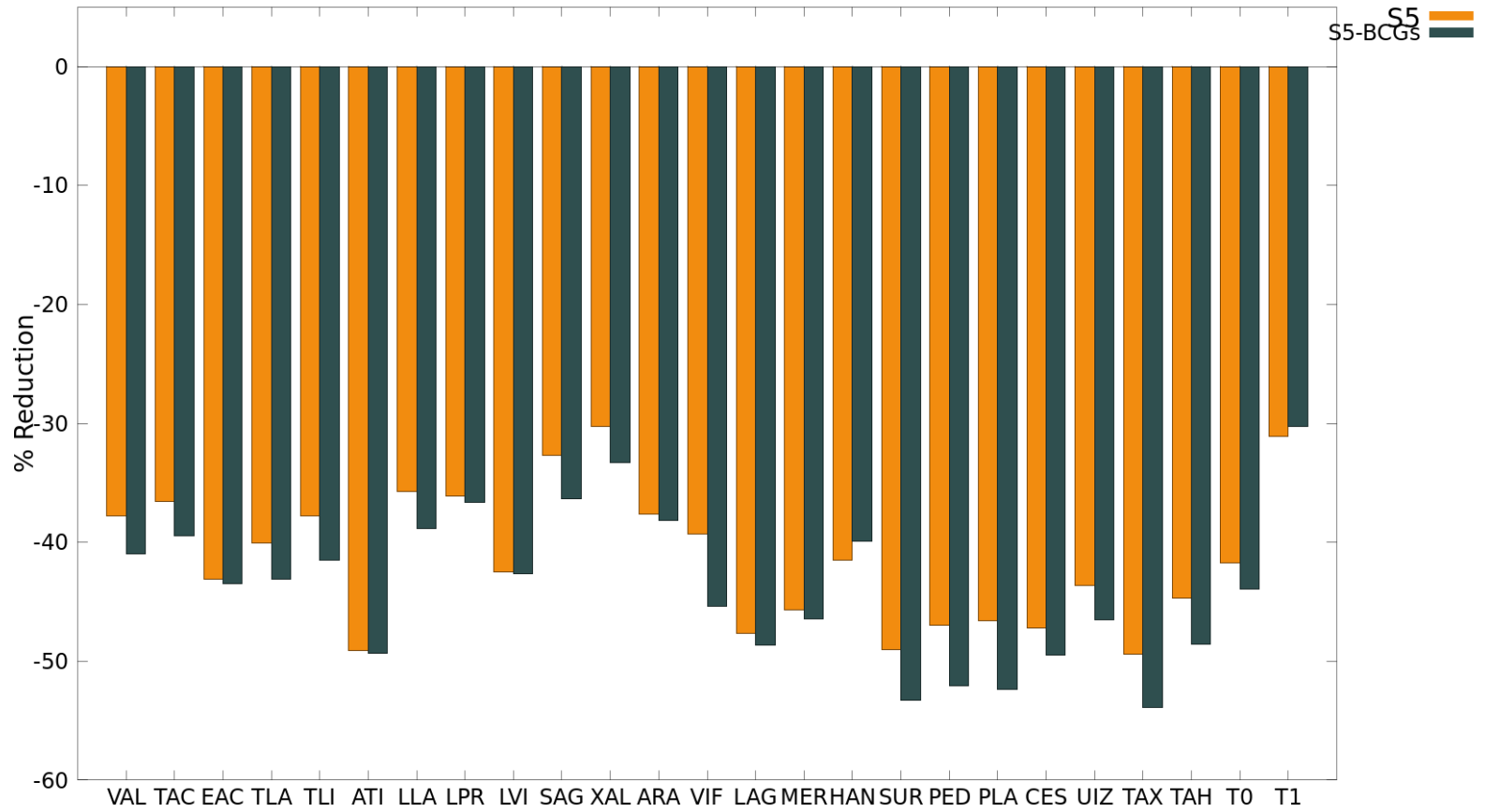
1
2 **Figure 4. PM₁ Sulfate concentration on 26 March at 16:00 LST after considering the**
3 **direct and indirect aerosol effects.**
4



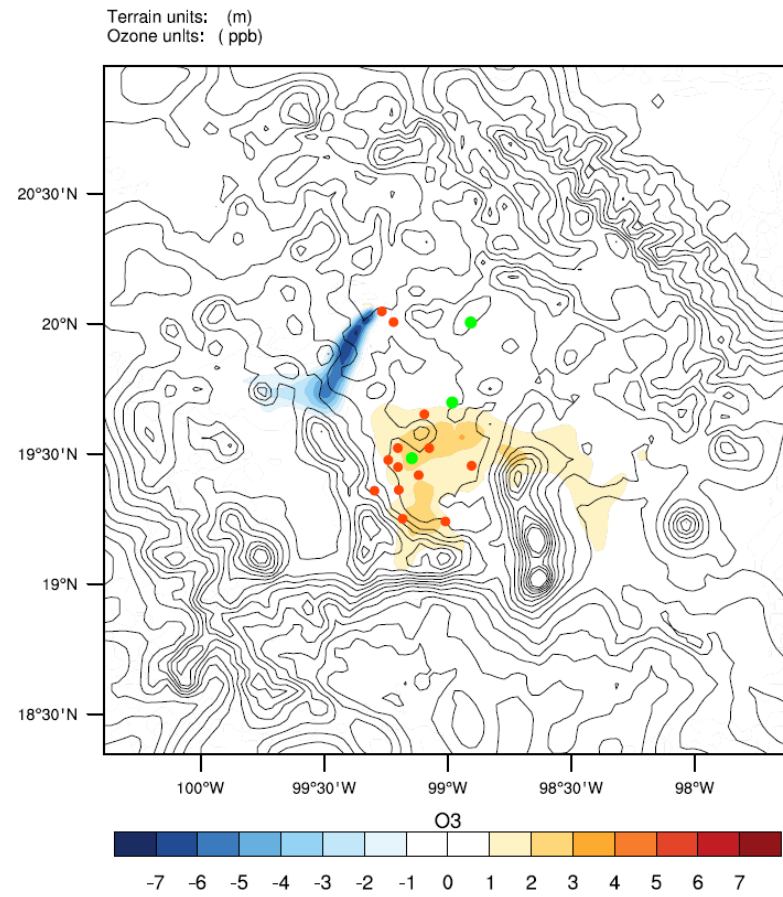
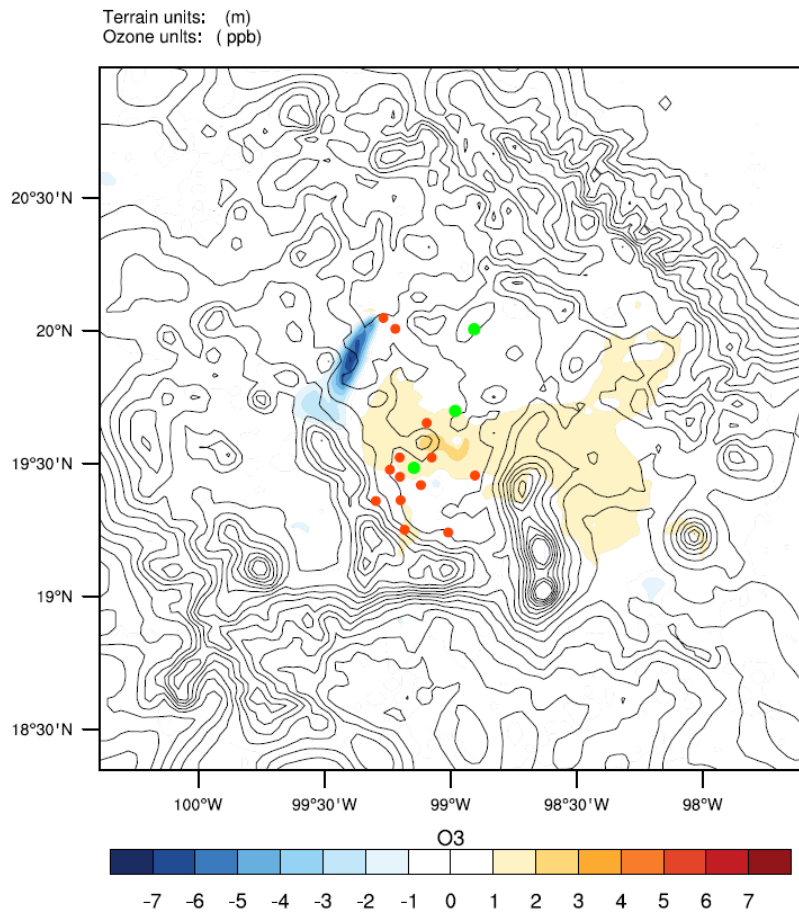
1 **Figure 5. Contribution of TIC, MCMA and cement plants on average SO₂**
 2 **concentration. Original results (top panel) and after including the aerosol chemistry**
 3 **with direct/indirect effects (bottom panel).**
 4



1
 2 **Figure 6. Model convergence zone that prevented the transport to the south on 24 March at 17:00 LST: simulation with**
 3 **aerosol phase plus direct and indirect effect (left panel); original results with gas phase (right panel). These plots show the**
 4 **streamlines (orange), and the wind vectors of some monitoring stations (purple). The filled circles denote supersites location**
 5 **(yellow).**
 6

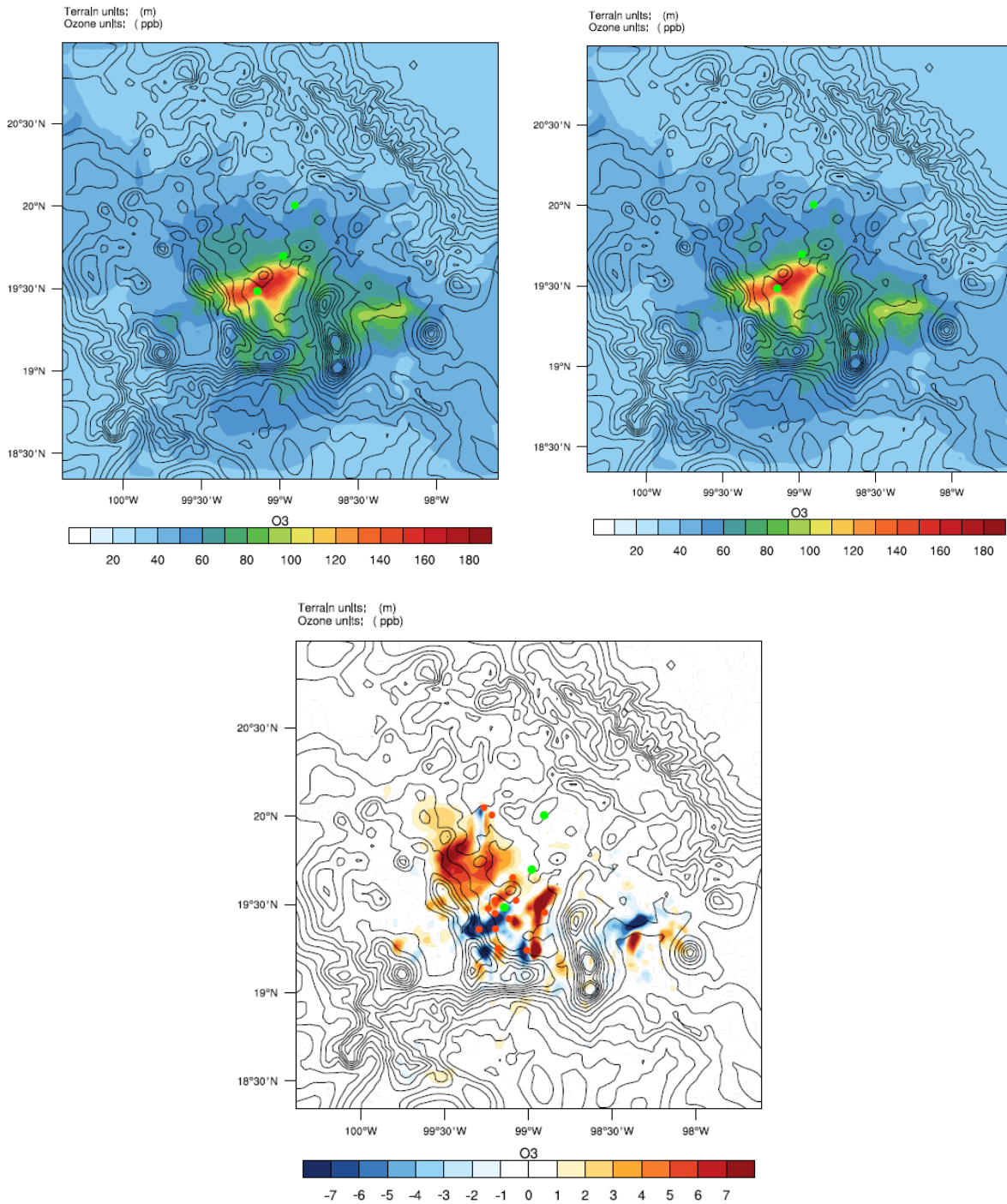


2
3 **Figure 7. Reduction scenario S5 after the inclusion of the aerosol phase (dark green) compared with the original results**
4 **(orange).**



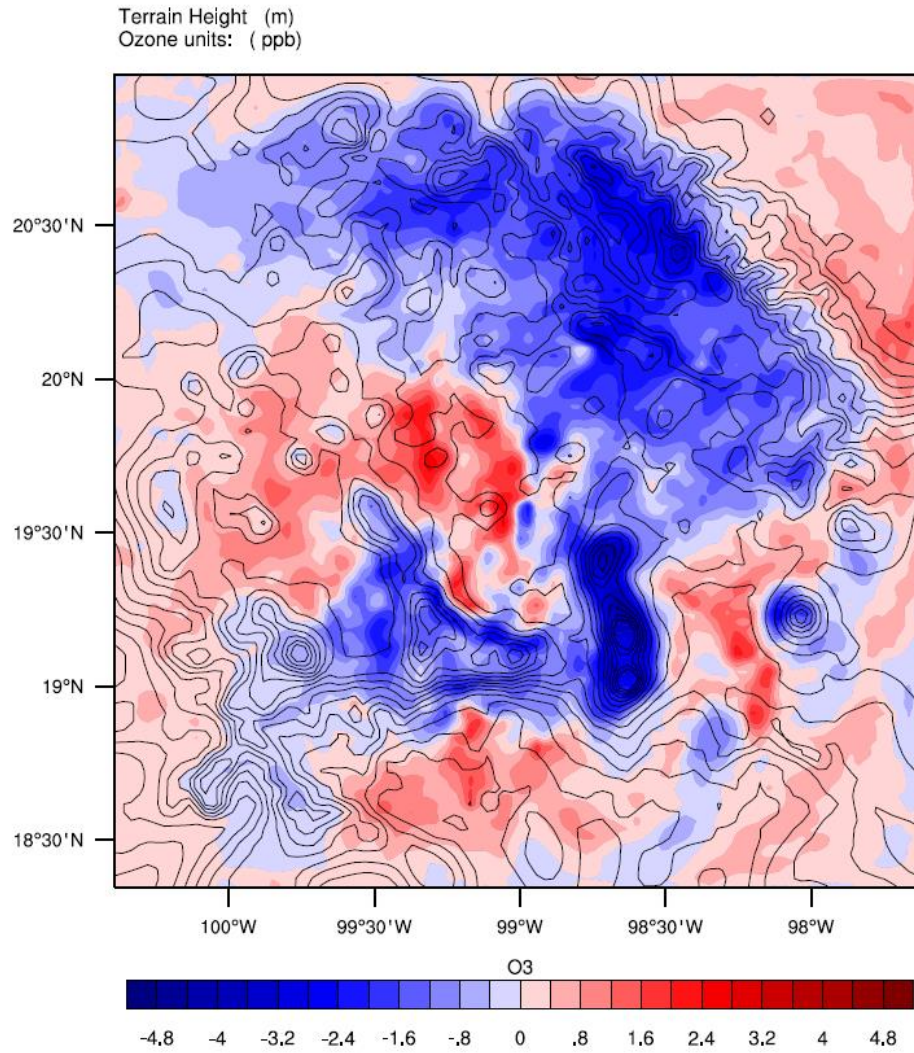
1 **Figure 8. Ozone plume from TIC-generated precursors on 25 March at 20:00 LST. Baseline case for gas phase using Dudhia**
 2 **scheme (left); Baseline case for gas phase using Goddard scheme (right).**

1

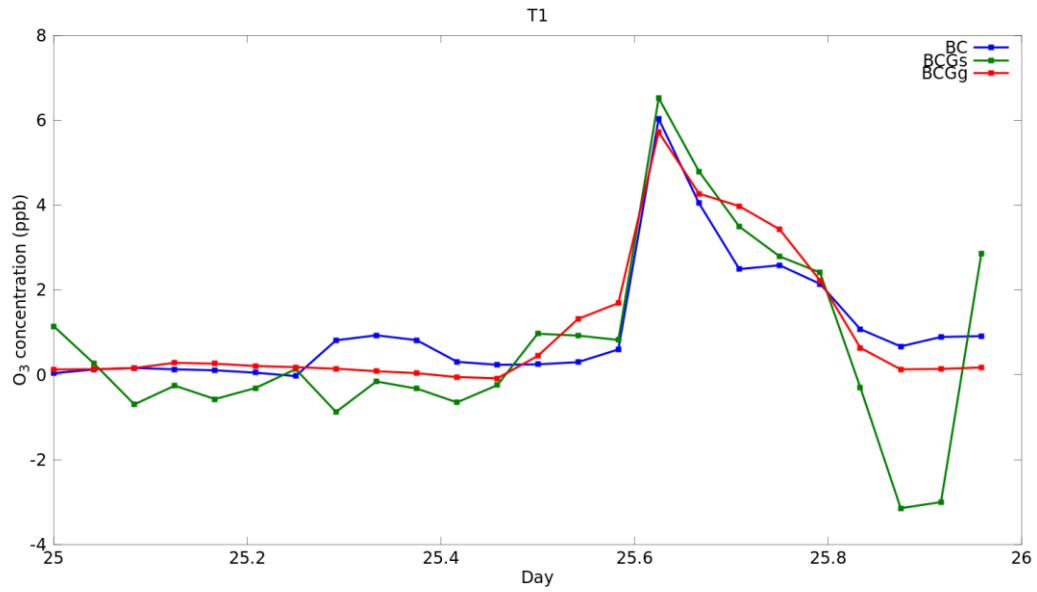


2

3 **Figure 9. Ozone plume from TIC-generated precursors after including the aerosol**
4 **phase plus the direct and indirect effects on 24 March at 15:00 LST. Baseline case**
5 **including all the anthropogenic sources (left); Simulation case with all the**
6 **anthropogenic sources but the TIC (right); Difference of concentration fields**
7 **(bottom).**



1
2 **Figure 10. Difference of the total average concentration for the entire simulation**
3 **period.**
4



1
 2 **Figure 11. Ozone concentration on 25 March at T1. Original Baseline case with gas**
 3 **phase (blue); Baseline case with Goddard scheme for gas phase (red); Baseline case**
 4 **with Goddard scheme including the aerosol phase plus direct and indirect effects**
 5 **(green).**

6
 7
 8